Biochimica et Biophysica Acta, 728 (1983) 394–402
Elsevier Biomedical Press

BBA 71573

ENHANCED HYDRATION OF DIPALMITOYLPHOSPHATIDYLCHOLINE MULTIBILAYER BY VINBLASTINE SULPHATE

LISBETH TER-MINASSIAN-SARAGA and GEORGETTE MADELMONT

Physico-Chimie des Surfaces et des Membranes, Equipe de Recherche du CNRS associée à l'Université Paris V, UER Biomédicale, 45 rue des Saints-Pères, 75270 Paris Cedex 06 (France)

(Received June 16th, 1982)
(Revised manuscript received October 4th, 1982)

Key words: Vinblastine sulfate; Dipalmitoylphosphatidylcholine; Multibilayer; Hydration change; Gel-liquid crystal transition

Vinblastine sulphate, an antimitotic and anti-inflammatory agent, modifies the thermal behaviour of the model membranes: the dipalmitoylphosphatidylcholine DPPC bilayers. The mixed DPPC and vinblastine sulphate multibilayers in the range of DPPC mole fraction 0.4 to 1 display clearly the gel-liquid crystal (chain melting) transition on the thermograms obtained with a differential scanning microcalorimeter. The molar enthalpy of this transition is slightly depressed by vinblastine sulphate (less than 10%). The temperature-composition phase diagram corresponds to a total insolubility of vinblastine sulphate inside the frozen (gel) bilayers and to a solubility of 0.2 (mole fraction) of vinblastine sulphate inside the fluid (liquid crystalline) bilayers. The dissolved vinblastine sulphate depresses the cooperativity number of the frozen ⇄ fluid transition of the bilayers very strongly (4- to 5-times). Up to its solubility concentration, vinblastine sulphate increases the amount of the structural water of the bilayers and modifies the thermal behaviour of this water. The 'expelled' vinblastine sulphate molecules are retained by the polar groups of DPPC molecules and screen their electrostatic interactions with the structural water molecules. Below 0°C, the amount of the structural water, which forms the aqueous separation between two bilayers, is enhanced by vinblastine sulphate. However, the drug reduces (screens) the bilayers interaction with the structural water molecules.

Introduction

Vinblastine sulphate is a lipophilic antitumor agent [1,2] with anti-inflammatory potency. It interferes with the metabolism of nucleic acids, proteins and lipids [3] and disrupts cell microtubules and microfilaments [4,5]. Vinblastine sulphate-activated membrane-associated enzymes may monitor the breakdown of membrane acidic phospholipids [6]. In this respect vinblastine sulphate has features in common with another lipophilic antiinflammatory drug, sulfindac [7.8]. Vinblastine sulphate, sulfindac and the antibiotic gramicidin S are large molecules (M_r around 1000) which affect only by a few percent the molar entropy of DPPC chain-melting transition [9,10] at all compositions. In contrast, the smaller cholesterol molecules [11,12] abolish this transition at relatively low concentrations. Therefore, we believe that cholesterol and the large drug molecules have different locations relative to the bilayers in the gel state.

In the present report we provide information on the effect of vinblastine sulphate on the hydration of DPPC/vinbastine sulphate bilayers at low temperature. This information is based on thermograms established with a differential scanning calorimeter within the temperature range $-60°C \leftrightarrow 50°C$ and on the interpretation of the low-temperature peaks described in Ref. 13. We find that vinblastine sulphate affects the bilayer hydration

more strongly than the molar entropy of the DPPC chain-melting transition.

Materials and Methods

Reagents

Vinblastine sulphate was a gift from Eli-Lilly (U.S.A.). DPPC was purchased from Fluka. Its purity was examined by thin-layer chromatography.

The samples were prepared as described in [10] using DPPC solutions in $CHCl_3/CH_3OH$ (9 : 1, v/v) and solid vinblastine sulphate. The dry mixture lipid plus drug weight was about 0.5 mg. To it was added 0.5 mg water and the mixture was weighed on a microbalance. The cup was sealed and incubated at 60°C for 32 h. A sealed reference cup containing 0.5 mg water was also prepared [12,13]. For each DPPC/vinblastine sulphate mixture studied, at least two samples were studied.

Thermograms

The DSC scanner was a Du Pont de Nemours thermoanalyser 990-910 equipped with a mechanical cooling accessory. Scanning was performed between −60°C and 50°C (above the DPPC chain melting transition). For each sample four heating and two cooling scans were carried out at a rate of 2 $K \cdot min^{-1}$. The sample and reference cups contained the same amount of water (see our technique [13]). Calibration of the apparatus is performed using the reference cup. The peaks areas were evaluated using a planimeter and the heats involved were deduced. The peaks limits are designated by the temperature at the origin of the peak, t_i, and at the peak maximum, t_m. As the heating, h, and cooling, c, modes display hysteresis, we note the temperatures t_{ih}, t_{ic}, t_{mh}, t_{mc} for each DPPC/vinblastine sulphate mixture. The composition of the bilayers is expressed as mole fraction of DPPC, x_{DPPC}, in the dry mixture. The amount of water, 0.5 mg, corresponds to 50% (w/w) of the wet system.

The thermograms displayed high-temperature peaks located above 30°C (Fig. 1a) and low-temperature peaks located below 0°C (Fig. 1b). The high-temperature peaks correspond to the well-known DPPC chain-melting process. From the measured heat of transition, the molar enthalpy of DPPC chain melting has been deduced, ignoring the presence of vinblastine sulphate. The sharp exothermic low temperature peaks at 0°C (in Fig. 1b) correspond to Q^r, the heat of ice melting inside the reference cup. It has been explained in Ref. 13 that Q^r divided by the molar enthalpy of pure ice melting, $L_o = 1.44$ $kcal \cdot mol^{-1}$, provides the mass, m_s, of the structural water between the phospholipid bilayers of a lamellar phase. This quantity is compared to similar ones obtained from X-ray diffraction studies [14].

The broad endothermic low-temperature peaks observed on the thermograms in Fig. 1b correspond to Q^s the heat of melting of frozen water inside the sample cups. According to Ref. 13, this structural water, which is dispersed and stabilised between the bilayers, is strongly perturbed by the surface forces emerging from the bilayer molecules. The broad low temperature endothermic peaks have been analysed following [13] and the results obtained are discussed below.

Results

Fig. 1 represents the thermograms obtained on cooling and heating the various fully hydrated DPPC/vinblastine sulphate lamellar mixtures. The compositions for which x_{DPPC} equals 1, 0.9, 0.8, 0.7, 0.6, 0.5, 0.4 and 0 have been studied. The high-temperature peaks are reproduced in Fig. 1a. In Fig. 1b we show the peaks located around 0°C.

High-temperature results (Fig. 1a)

Thermogram and heat of transition. The pretransition peak of DPPC, centred around 33°C, is observed only for the heating mode of pure DPPC. The molar enthalpy of this transition is equal to 1.7 $kcal \cdot mol^{-1}$. The temperature of the main transition is inside the range 40.5–41°C. The corresponding molar enthalpy is equal to 8.2 $kcal \cdot mol^{-1}$. The total molar enthalpy of transition is equal to 9.9 $kcal \cdot mol^{-1}$. These results are consistent with previously reported ones for the heating runs [2].

We have obtained additional information by comparing the heating and the cooling mode thermograms.

Heating mode. The peak onset in the heating mode thermogram at the temperature t_{ih} is located

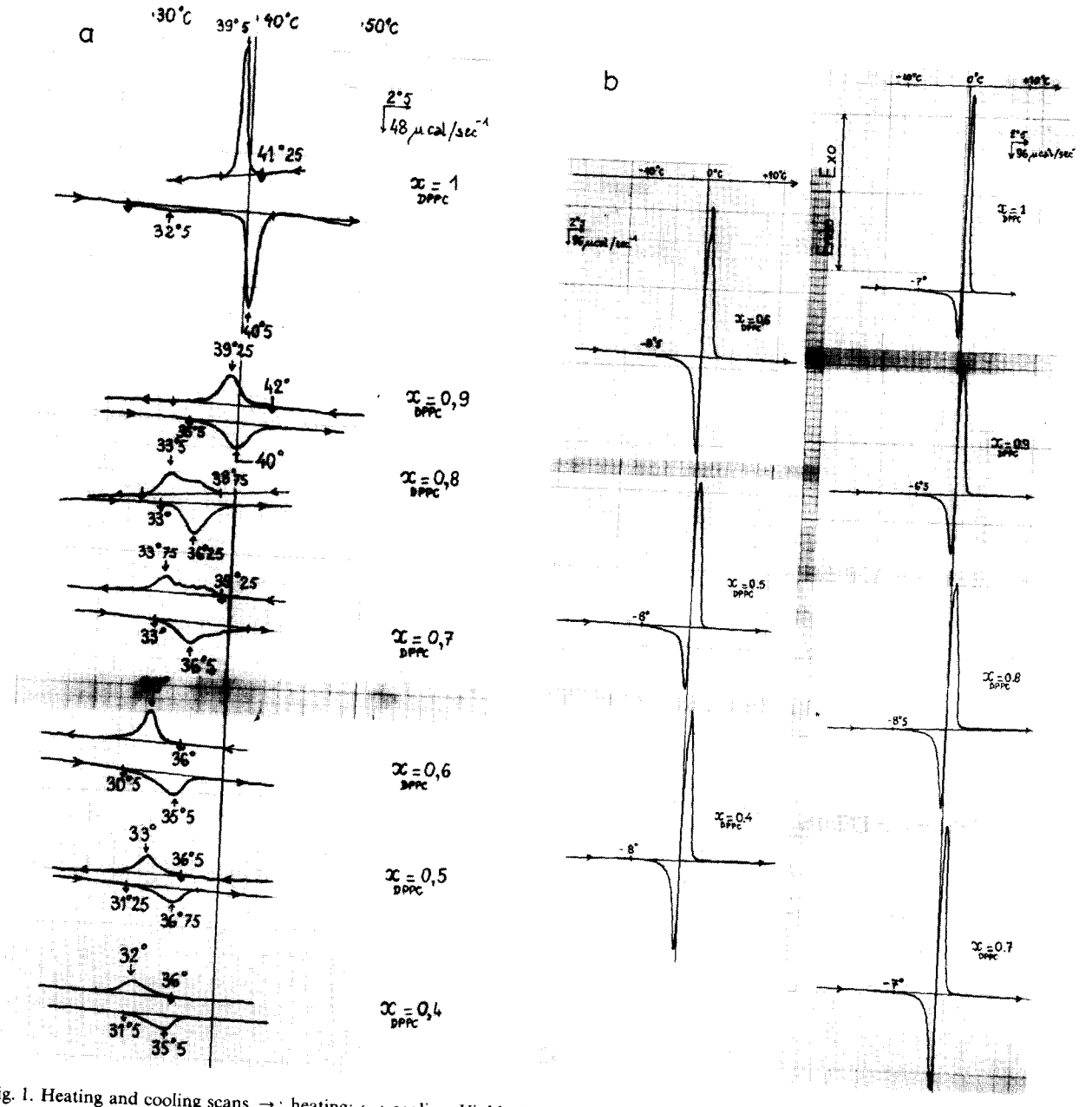

Fig. 1. Heating and cooling scans. →: heating; ←: cooling. Vinblastine sulphate + DPPC + H_2O (50%, w/w). x_{DPPC} = mole fraction of DPPC in the dry mixture. (a) High temperature peaks. Peak onset and peak maxima temperature as indicated. (b) Low temperature peaks. The maximum depression, $\hat{t}_{max}$, is indicated.

on the solidus line. The peak maximum at the temperature t_{mh} is located on the liquidus line and corresponds to the end of the DPPC transition. For x_{DPPC} equal to 1, 0.9, 0.8, 0.6, 0.5, 0.4 in Fig. 1a only one peak is displayed in the heating mode thermograms (Fig. 1a). We assume that the temperature range $\Delta t_h = t_{mh} - t_{ih}$ corresponds to a 'complete' (approx. 100%) transition of the bilayers.

Cooling mode. The peak onset for the cooling mode at t_{ic} is located on the liquidus line. Peak maximum at t_{mc} is located on the solidus line. For

x_{DPPC} equal to 1, 0.9, 0.6, 0.5 or 0.4, the cooling mode thermograms display one peak. The temperature range $\Delta t_c = t_{ic} - t_{mc}$ is assigned to a 'complete' (approx. 100%) transition of the bilayers.

Mechanical and thermal relaxations in the DSC device occur beyond t_{mc} and t_{mh}.

In Fig. 1a, the solidus and the liquidus temperature limits thus defined are shown. Except for the mixtures with $x_{DPPC} = 0.7$ and $x_{DPPC} = 0.8$ each limit displays up to 2 K hysteresis between cooling and heating modes. For pure DPPC ($x_{DPPC} = 1$) t_{mh} is at 40.5°C and t_{ic} is at 41.25°C. For $x_{DPPC} = 0.9$ we have $t_{mh} = 40$°C and $t_{ic} = 42$°C. For x_{DPPC} equal to 0.6 or 0.4 the hysteresis is only about 0.5 K. The same type of hysteresis is displayed by the peak maxima t_{mc} and the low-temperature limit t_{ih} (see the values in Fig. 1a). Inside the transition range $0.7 > x_{DPPC} > 0.8$ the peak is a superposition of peaks of the type observed for either $x_{DPPC} > 0.9$ or $x_{DPPC} < 0.6$.

In Fig. 2a and b, the solidus, t_{ih}, t_{mc}, and liquidus, t_{mh}, t_{ic}, lines are drawn separately. The hysteresis is smaller (1–2 K) for the solidus line than for the liquidus line (1–3 K). The curvatures of the two lines are similar. Both lines display a sharp change (4–5 K) in the interval $0.8 < x_{DPPC} < 0.9$ and a plateau for $x_{DPPC} < 0.7$.

The average transition temperature range Δt_h and Δt_c for the heating and for the cooling modes, respectively, are calculated from Fig. 2a and b. For pure DPPC, their values are small: $\Delta t_h = 1.0$ K $\pm$ 0.5 and $\Delta t_c = 1$ K $\pm$ 0.5. For $x_{DPPC} = 0.9$ or 10 mol% vinblastine sulphate in one thermogram only, the peak onset for the cooling mode was above the maximum temperature, t_{mh}, for the heating mode. At this composition, $\Delta t_h \approx 4$ K $\pm$ 1.5 and $\Delta t_c \approx 2.5$ K $\pm$ 1.5. We did not decompose the broad peaks obtained at the intermediate compositions x_{DPPC} equal to 0.7 or 0.8 which seem to be representative of a complex structure intermediate between those of the vinblastine-sulphate-poor ($x_{DPPC} > 0.9$) and vinblastine-sulphate-rich ($x_{DPPC} < 0.7$) samples.

Values of t_{mh}, t_{mc}, Δt_c are reported in Table I.

The molar enthalpy of DPPC chain melting, ΔH_{DPPC}, is obtained from the total area of the high-temperature broad peaks. The values obtained for the cooling and heating mode scans are shown in Fig. 2c. Neither the mode of scanning

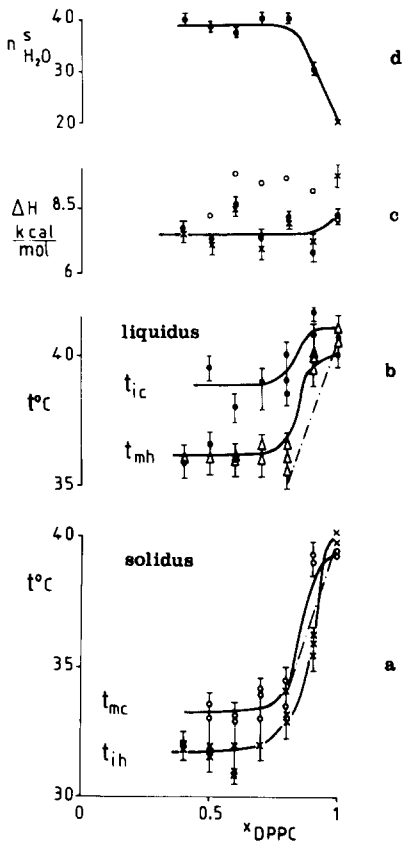

Fig. 2. Transition temperatures, molar enthalpy and amount of structural water. DPPC + vinblastine sulphate + H_2O (50%, w/w). x_{DPPC} = mol fraction of DPPC for the dry mixture. t = transition temperature. (a) Solidus line. t_{ih}, t_{ic} = peak onset and peak maximum temperatures on heating, h, and on cooling, c, scans. (b) liquidus line. t_{ic}, t_{mh} = peak onset and peak maximum temperatures on cooling, c, and heating, h, scans. (c) ΔH_{DPPC} = molar enthalpy for the DPPC gel ⇄ liquid crystalline transition. ×, cooling scan; ○, heating scan [10]. ●, heating scan (present experiments). (d) $n^s_{H_2O}$: amount of structural water [(H_2O)/(DPPC + vinblastine sulphate)] (mol/mol).

nor vinblastine sulphate affects very significantly ΔH_{DPPC}, which is on the average equal to 7.5 $\pm$ 1 kcal · mol^{-1} or less than 1 kcal · mol^{-1}, smaller than ΔH_{DPPC} of pure DPPC.

The corresponding molar entropy of DPPC chain melting, $\Delta S_{DPPC} = [\Delta H_{DPPC}/T_{ih}]$ is reduced by vinblastine sulphate from $\Delta S^\circ_{DPPC} = 26.1$ e.u. · mol^{-1} * for pure DPPC to $\Delta S_{DPPC} = 24.6$ e.u. · mol^{-1}. This variation is small: 6% of ΔS°_{DPPC}.

* e.u., cal · K^{-1}.

TABLE I

TEMPERATURE AND COOPERATIVITY NUMBER FOR THE GEL TO LIQUID CRYSTAL TRANSITION OF DPPC

x_{DPPC}: mole fraction in the dry DPPC/vinblastine sulphate mixture. 50% (w/w) hydration. ΔT, range of temperature for 'complete' (approx. 100%) transition. T, transition temperatures. h, c: heating, cooling modes. ΔH_{vH}, van 't Hoff enthalpy for the cooperative transition. n: cooperativity number for the transition (see Eqn. 5). $\Delta H_{cal} = 8.2$ kcal·mol^{-1} (main transition, heating mode) and $\Delta H_{cal} = 9.9$ kcal·mol^{-1} (main transition + pretransition, cooling mode) for $x_{DPPC} = 1$. For $x_{DPPC} \neq 1$, $\Delta H_{cal} = 7.5$ kcal·mol^{-1} for both cooling and heating modes (see Fig. 2c).

x_{DPPC}	ΔT_h (K)	T_h (K)	ΔT_c (K)	T_c (K)	ΔH_{vHh} (kcal/mol)	ΔH_{vHc} (kcal/mol)	n_h	n_c
1	1.0	313.65	1	313.65	1558	1558	190	158
0.9	4.0	311.65	2.5	311.15	384	614	52	82
0.7	4.0	308.15	5.0	306.45	376	296	50	38

The presently reported values of ΔH_{DPPC} in the range $0.6 < x_{DPPC} < 0.9$ are smaller by about 2 kcal·mol^{-1} than those reported in Ref. 10. The history of the samples studied in Ref. 10 is different from that of the presently studied ones. Those samples were never cooled below 0°C and were not incubated at 60°C for 16 h, as opposed to those presently studied.

Low temperature peaks (Fig. 1b)

The mass, m_s, of the water dispersed by the bilayers is obtained from the (apparently) exothermic peaks of the thermograms shown in Fig. 1b as explained in Materials and Methods and in Ref. 13. The quotient $n^s_{H_2O} \propto m_s/N'$, where N', the total number of DPPC plus vinblastine sulphate bilayer molecules, is the average number of structural water molecules per molecule inside the sample. Its variation with x_{DPPC} is shown in Fig. 2d. For $x_{DPPC} > 0.8$, $n^s_{H_2O}$ is independent of the bilayer composition.

The low-temperature endothermic peak corresponds to the heat of melting, Q^s, of the frozen structural water of mass m_s. As shown in Ref. 13, $Q^s < Q^r$, the heat involved in the metling of the mass, m_s, of pure ice. The difference $\Delta Q = Q^r - Q^s$ is interpreted according to Ref. 13.

In Ref. 13 we suggest the following analytical expression for the endothermic peaks within the temperature range $-10°C < t < -1°C$ (see Fig. 1b).

$$\varepsilon(t) \simeq \dot{T}_p \frac{m_s L}{18\alpha} \left\{ \frac{\varnothing(L,l)}{2} \left(-\hat{T}_{min}\right) \right\}^{1/\alpha} \left(-\hat{T}\right)^{-(\alpha+1/\alpha)} \quad (1)$$

where $\varepsilon(t)$ is the deflection from the base line at t, $\dot{T}_p = 2$ K·min^{-1} is the rate of scanning, $L \neq L_o$ is the effective molar enthalpy of frozen structural water, $\alpha = 2$, L and $l(t)$ are, respectively, the thicknesses of the aqueous gap separating two bilayers [14] and of the unfrozen water layer at the temperature t, $\varnothing(L, l)$ ($\rightarrow 1$ for $l \rightarrow L$) is a geometrical factor and $\hat{T} = T - T_o$ is the shift of the temperature from the normal ice-melting temperature $t_o = 0°C$. The maximum deflection, $\varepsilon_{max}(\hat{T}_{min})$, occurs at the smallest shift $|\hat{T}_{min}|$. Eqn. 1 is tested in Fig. 4 using the results of Fig. 1b and of various other thermograms (not shown). Although the experimental reproducibility of the thermograms is not excellent, a given peak appears to be represented quite well by Eqn. 1 for $|\hat{T}| > 1$ K. For $|\hat{T}| \rightarrow 0$ the error, 0.25 K, in $\hat{T}$ is too large. Therefore, $(-\hat{T}_{min})$ is obtained by extrapolating the

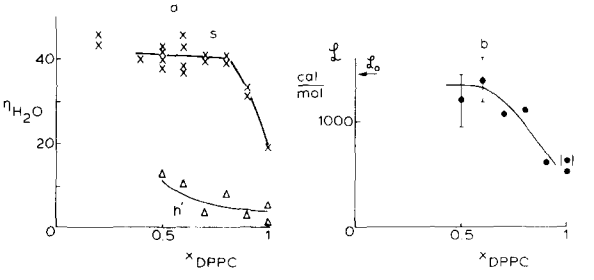

Fig. 3. Thermal behaviour of structural water in DPPC/vinblastine sulphate hydrated multibilayers. x_{DPPC} = mole fraction of DPPC inside the dry mixture. (a) Structural water, and non-freezing water, h'. n_{H_2O} = [H_2O/(DPPC + vinblastine sulphate)](mol/mol). (b) Molar enthalpy of melting of the frozen structural water inside multibilayers, L, and in bulk water, $L_o = 1440$ cal·mol^{-1}.

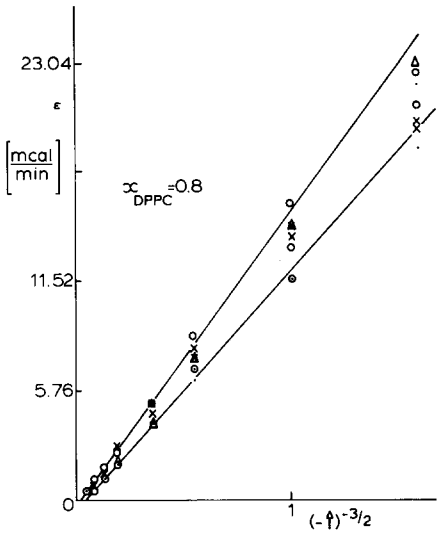

Fig. 4. Test of Eqn. 1 using the data of Fig. 1b. ε, rate of heat input. $\hat{T} = T - 273.15$ K = temperature shift from 0°C. x_{DPPC} = mole fraction of DPPC inside the dry DPPC/vinblastine sulphate mixtures as indicated. Results of seven temperature scans. The lines show the scattering of the slope and of enthalpy of (frozen water) melting values.

lines in Fig. 4 to the values of ε_{max} read on the thermograms shown in Fig. 1b. A second parameter ($-\hat{T}_{max}$) is obtained by extrapolating the lines in Fig. 4 to $\varepsilon(\hat{T}_{max}) = 0$. Values of $\hat{T}_{max}$ are indicated in Fig. 1b. The effective values of L are found from the slopes of lines such as those shown in Fig. 4 using Eqn. 1. They are plotted vs. x_{DPPC} in Fig. 3b. The value of L for pure DPPC is 15% smaller than the value reported in Ref. 13 and quoted in Fig. 3b (0.52 instead of 0.640 kcal · mol^{-1}). This difference is within the limits of thermogram reproducibility. Athough the scatter of the values of L is important, the increase of L by vinblastine sulphate incorporation is significant. It is parallel to the increase of the amount of structural $n^s_{H_2O}$. For a 1/1 molecular ratio DPPC/vinblastine sulphate, L becomes comparable to L_o.

It has been shown in Ref. 13 that the heat Q^s involved in the melting of the frozen structural water may be expressed as follows:

$$Q^s = \frac{m_s L}{18}\left(1 - \frac{2l_o}{L}\right) \qquad (2)$$

where l_o is the minimum thickness of the non-freezing (liquid) structural water. As $L \propto n^s_{H_2O}$ using Eqn. 2 and the measured values of Q^s, m_s and L $(l_o/L) = (n^{h'}_{H_2O}/n^s_{H_2O})$ is evaluated. We plot in Fig. 3a (line h') the variation of $n^{h'}_{H_2O}$ with x_{DPPC}. It parallels that of L with x_{DPPC}. Therefore, according to our approach, the amount of structural and of non-freezing water and the molar enthalpy and entropy of melting of the frozen structural water of DPPC bilayers are affected by vinblastine sulphate.

Discussion

Vinblastine sulphate is a dimeric alkaloid (Fig. 5) of molecular weight 909.1 g · mol^{-1}. Its partition coefficient, P, between octanol and water at room temperature being equal to log $P = 3.65$, vinblastine sulphate is considered lipophilic. Nevertheless, the vinblastine sulphate solubility in water at room temperature may be as high as approx 0.1 M (communicated by Eli Lilly). On heating the aqueous solutions, vinblastine sulphate undergoes reversible thermal aggregation to an extent which is dependent on pH and vinblastine sulphate concentration. The aggregation, which may be prevented by excess anionic detergent or proteins [15], is assigned to vinblastine sulphate lipophilic character and it may be expected that vinblastine sulphate molecules penetrate deeply inside the DPPC bilayers.

The results of ΔH_{DPPC} in Fig. 2c show clearly that vinblastine sulphate does not perturb either the melting or the freezing of DPPC chains significantly. The molar enthalpy of this transition is lowered by about 12% and the corresponding ent-

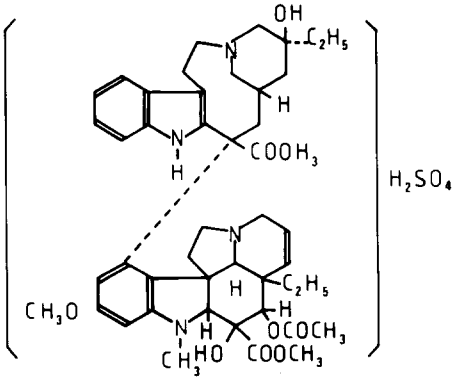

Fig. 5. Molecular structure of vinblastine sulphate.

ropy by about 6%. The significant depression of the gel → liquid crystal (G → LC) transition temperature for DPPC indicates (Fig. 2a, b) that the drug does affect the free energy of DPPC. It enhances also the average amount of structural water $n^{s}_{H_2O}$ of the frozen lamellar phase (Fig. 2d), i.e., it increases the aqueous separation between bilayers.

As a first approximation, we analyze the results shown in Fig. 2a and according to Hill [16] which suggested for such phase diagrams the following expression:

$$\frac{1}{T_{DPPC}} - \frac{1}{T} = \frac{R}{\Delta H_{DPPC}} \ln \frac{x^{LC}_{DPPC}}{x^{G}_{DPPC}} \tag{3}$$

where $R = 1.98$ e.u. $\cdot$ mol^{-1}, T, T_{DPPC} are transition temperatures for the mixed vinblastine sulphate/DPPC and for the pure DPPC bilayers, x^{LC}_{DPPC} and x^{G}_{DPPC} are the DPPC mole fractions inside the fluid or the frozen bilayers. Both x^{LC}_{DPPC} and x^{G}_{DPPC} are monitored by vinblastine sulphate concentration inside the aqueous regions. Eqn. 3 with $x^{G}_{DPPC} = 1$ and $\Delta H_{DPPC} = 8$ kcal $\cdot$ mol^{-1} satisfies the solidus band (see calculated line in Fig. 2a). In contrast, the liquidus band in Fig. 2b would correspond to the phase diagram, Eqn. 3, provided either $x^{G}_{DPPC} < 1$ or $a^{LC}_{DPPC} > x^{LC}_{DPPC}$, the activity of DPPC in the liquid crystalline state, is increased by vinblastine sulphate. The possibility $a^{LC}_{DPPC} > x^{LC}_{DPPC}$ is consistent also with the non-significant effect of vinblastine sulphate on ΔH_{DPPC} (Fig. 2c). Such a non-significant effect of the incorporated large lipophilic molecules has been noticed for other two lipophilic large molecules: gramicidin S [9] and the anti-inflammatory agent sulindac sulfide [7,8].

Both depressions of the liquidus and of the solidus temperatures saturate at $x_{DPPC} \approx 0.8$ and point to the limited miscibility of vinblastine sulphate and DPPC when $x_{\text{vinblastine sulphate}} > 0.2$ inside the sample.

Eqn. 3 implies that the mixed DPPC + vinblastine sulphate bilayers form very large ordered domains displaying highly cooperative transitions. For them, unless complexes between vinblastine sulphate and DPPC are formed, only depressions of DPPC transition temperature would be observed. This is verified by all the heating mode thermograms. In contrast, some of the cooling mode thermograms for the poor ($x_{DPPC} = 0.9$) vinblastine sulphate samples display a small increase in the transition temperature on the liquidus line, but not on the solidus line. This increase may be due to the broadening of the DPPC transition peak involved by the decrease in the cooperativity of this transition [17]. Based on this observation, we discard the assumption of complex formation and evaluate the index of cooperativity, n, for the transition as defined in Ref. 1. If ΔH_{vH} is the relevant van 't Hoff enthalpy for a 'complete' (100%) pure two-state order ⇄ disorder transition, by definition we have:

$$\Delta H_{vH} = 4R^2_{Tm}\left(\frac{d\alpha}{dT}\right)_{T_m} \approx \frac{8RT^2_m}{\Delta T} \tag{4}$$

where $(d\alpha/dT)_{T_m}$ is the maximum rate of the transition, α is the degree of advancement of the transition and $T_m = T(\alpha = 0.5)$. As $(d\alpha/dT)_{T_m} \approx 2/\Delta T$, where ΔT is the temperature range corresponding to the complete transition we evaluate the cooperativity number, n, defined in Ref. 17 as follows:

$$n = \frac{\Delta H_{vH}}{\Delta H_{cal}} \tag{5}$$

The values of $\Delta H_{cal} \equiv \Delta H_{DPPC}$ are reported in Fig. 2c. From [2,5] and the values of ΔT_h, ΔT_c, T_{mh}, T_{mc} reported in Table I we evaluate n_h and n_c for the cooling and the heating mode transitions. The results obtained are reproduced in Table I (last two columns). It is evident that vinblastine sulphate perturbs the DPPC bilayers and reduces by 4 to 5 times the cooperativity number of the DPPC liquid crystal ⇄ transition. For pure DPPC, the values we obtained for n are of same order as those reported in Ref. 15. The difference might be the consequence of our approximation (see Eqn. 4). However, the modulation of n by vinblastine is significant (see Table I).

The difference between n_c and n_h is within the (large) experimental error on ΔT. For $x_{DPPC} = 0.9$ the difference between n_h and n_c is significant. As for the depression of the transition temperature, the depression of the DPPC transition cooperativity number by vinblastine sulphate saturates at $x_{DPPC} < 0.8$.

We may speculate about this limited miscibility or solubility of vinblastine sulphate knowing the overall composition of the sample at $x_{DPPC} = 0.8$. The sample contains approx. 50 μg vinblastine sulphate, 500 μg H_2O and approx. 450 μg DPPC. Ignoring DPPC, the concentration of vinblastine sulphate in water alone would be approx. 0.2 M, or twice its solubility in water. In the presence of fluid DPPC bilayers, solubilization of vinblastine sulphate would lower its concentration in water. If at $x_{DPPC} = 0.8$ either the aqueous space or the bilayer becomes saturated with vinblastine sulphate, for $x_{DPPC} < 0.8$, the sample would contain pure (excess) undissolved vinblastine sulphate and x^{LC}_{DPPC} and the depression, $T_{DPPC} - T$, would become constant, too.

Furthermore we note that both the amount (Fig. 3a) and the thermal behaviour (Fig. 3b) of the structural water also become independent of vinblastine sulphate for the vinblastine-sulphate-saturated bilayers ($x_{DPPC} < 0.8$). In these bilayers, on the one hand the amount of the structural water has doubled compared to the amount of structural water in pure DPPC bilayers; on the other hand, the molar enthalpy of melting, L, of this frozen water has increased almost to the value, L_o, for bulk ice. The evolution of $n^{h'}_{H_2O}$ (Fig. 3a) is not clear, the results being too scattered. The increase in the average hydration number $n^{h'}_{H_2O}$ by vinblastine sulphate (Fig. 3a) contrasts with the saturation observed for the depression of gel $\rightleftarrows$ liquid crystal transition temperature and cooperativity (Fig. 2a, Fig. 2b and Table I). It contrasts also with the constant value of ΔH_{DPPC} (Fig. 2c). We suggest that the undissolved (excess) vinblastine sulphate present in the samples at $x_{DPPC} < 0.8$ hydrates too and contributes in an unpredictable way to the average value of $n^{h'}_{H_2O}$. Further studies carried out at increasing overall hydration of the samples might elucidate the effect of vinblastine sulphate on $n^{h'}_{H_2O}$.

Conclusion

The gel $\rightleftarrows$ liquid crystalline transition of DPPC multibilayers is not abolished by the incorporated vinblastine sulphate molecules under our present experimental conditions. Except for a small temperature lag hysteresis possibly orginating in the relatively high (2 K · min^{-1}) scanning rate, heating and cooling scans provided similar thermograms demonstrating the high reversibility of the gel $\rightleftarrows$ liquid crystal transitions. Vinblastine sulphate depresses the molar enthalpy of this transition ΔH_{DPPC} by about 12%, while the transition temperature and cooperativity number, n, are strongly depressed.

The phase diagram, $t - x_{DPPC}$, based on these results indicates that the frozen (gel) bilayers of DPPC expel the vinblastine sulphate molecules incorporated by the fluid DPPC bilayers. The about 12% decrease of ΔH_{DPPC} by vinblastine sulphate might correspond to either a small ordering of DPPC fluid chains or a small disordering of DPPC frozen bilayers slightly contaminated by vinblastine sulphate.

While the frozen paraffin chains of DPPC molecules expel the vinblastine sulphate molecules, their (DPPC) polar groups may attract them electrostatically. This has been assumed before for the large lipophilic molecules of gramicidin S incorporated inside the DPPC multibilayers [9]. In this position the vinblastine sulphate molecules might screen the electrostatic interactions between the DPPC polar groups and the structural water molecules and increase the width of the aqueous spacings between the bilayers.

Our results verify this expectation. The molar enthalpy for the structural water melting increases towards its value in bulk and the amount, $n^{s}_{H_2O}$, of the structural water, proportional to the width of the aqueous spacings, increases also when the molar ratio vinblastine sulphate/DPPC is increased. We may speculate that the resulting increasing distance between successive bilayers reduces the (molecular) correlation between the DPPC molecules in both the gel and liquid crystalline state and reduces too the cooperativity of the transition. This evolution is expressed by the large drop (4–5-times) in the value of the cooperativity number, n.

The effect of vinblastine sulphate on several properties of DPPC bilayers saturates for $x_{DPPC} < 0.8$. These properties are: the downward shift for the gel $\rightleftarrows$ liquid crystal transition temperature and for the cooperative number and the upward shift for the amount and melting enthalpy of the structural water. We conclude that the composition,

$x_{DPPC} = 0.8$, equivalent to the molar ratio 1 vinblastine sulphate/4 DPPC, corresponds to the limit of miscibility of vinblastine sulphate with DPPC in the fluid state under the present experimental conditions.

Our studies are relevant to pharmaceutics and cancer chemotherapy by liposomally encapsulated vinblastine sulphate [18,19]. The liposome stability during lyophilization and during liposome adhesion to cell membranes may be controlled by their structural water as stated elsewhere [12,13,14,20]. To obtain information on this structural water, our original DSC approach is very useful.

Acknowledgment

Partial support from the PIRMED (Centre National de la Recherche Scientifique) under the grant No. ASP 6107 is gratefully acknowledged.

References

1 Neuss, N. (1963) Bull. Soc. Chim. France, 1509–1516
2 Johnson, I.S., Armstrong, J.G., Gorman, M. and Burnett, J.P. (1963) Cancer Res. 23, 1390–1427
3 Creasey, W.A., Bensch, K.G. and Malawista, S.E. (1971) Biochem. Pharmacol. 20, 1579–1588
4 Owellen, R.J., Owens, A.H. and Donigian, D.W. (1972) Biochem. Biophys. Res. Commun., 47, 685–691
5 Owellen, R.J., Donigian, D.W., Hartke, C.A. and Hains, F.O. (1979) Biochem. Pharmacol. 26, 1213–1219
6 Schroeder, F., Fontaine, R.N., Feller, D.J. and Weston, K.G. (1981) Biochim. Biophys. Acta 643, 76–88
7 Fan, S.S. and Shen, T.Y. (1981) J. Med. Chem., 24, 1197–1202
8 Hwang, S.B. and Shen, T.Y. (1981) J. Med. Chem., 24, 1202–1211
9 Pache, W., Chapman, D. and Hillaby, R. (1972) Biochim. Biophys. Acta 255, 358–364
10 Ter-Minassian-Saraga, L., Madelmont, G., Hort-Legrand, C. and Métral, S. (1981) Biochem. Pharmacol. 30, 411–415
11 Ladbrooke, B.D., Williams, R.M. and Chapman, D. (1968) Biochim. Biophys. Acta 150, 333–340
12 Ter-Minassian-Saraga, L. and Madelmont, G. (1982) FEBS Lett. 137–140
13 Ter-Minassian-Saraga, L. and Madelmont, G. (1982) J. Colloid Interface Sci. 85, 375–388
14 Le Neveu, D., Rand, R.P. and Parsegian, V. (1976) Nature 259, 601–603
15 Nimni, M.E. (1972) Biochem. Pharmacol. 21, 485–493
16 Hill, M.W. (1974) Biochim. Biophys. Acta 356, 117–124
17 Hinz, H.J. and Sturtevant, J.M. (1972) J. Biol. Chem. 247, 6071–6075
18 Layton, D., De Meyer, J., Collard, M.P. and Trouet, A. (1979) Eur. J. Cancer 15, 1475–1483
19 Layton, D. and Trouet, A. (1979) Eur. J. Cancer 15, 945–950
20 Ter-Minassian-Saraga, L. and Madelmont, G. (1981) J. Colloid Interface Sci. 81, 369–384